Mem. S.A.It. Vol. 84, 711

Memorie della

Fe Kα X-ray light echoes in AGN

A. Zoghbi[1,2]

[1] Department of Astronomy, University of Maryland. College Park, MD 20742-2421. USA
[2] Joint Space-science Institute (JSI). College Park, Maryland 20742-2421. USA
e-mail: `azoghbi@astro.umd.edu`

Abstract. Studies of X-ray reverberation from the environs of black holes has advanced significantly in the last few years. Reverberation lags were first seen between the direct emission and the reflected emission dominating the soft excess in some AGN. The delays are comparable to the light-crossing time at a few gravitational radii from the black hole. The later discovery of iron K reverberation band has lifted some ambiguities associated with the spectral identification of the soft excess. Such results, which are presented and discussed here, not just confirmed the interpretation of these lags, but also is allowing us to use a 'clean' part of the spectrum to better constrain the emission in the vicinity of the black hole.

Key words. Accretion, accretion disks – Black hole physics – X-rays: galaxies

1. Introduction

There are several lines of evidence that localize the X-ray radiation from active galaxies (AGN) to a very compact region close to the central black hole (BH). The bulk of the radiation in the X-ray band is emitted through Compton scattering producing a power-law component. The accreted material reflects some of the incident photons giving rise to a characteristic reflection spectrum (Ross & Fabian 1993). If the reflected emission originates very close to the black hole, relativistic distortions are imprinted in the spectra (Fabian et al. 1989), causing emission lines to be broadened and distorted.

The turbulent nature of the accretion and emission processes lead to a variable power-law component, which is often observed. The presence of a reflecting medium naturally leads to time delays (Reynolds et al. 1999), which encode information about the geometry of the emitting region.

The Narrow Line Seyfert 1 galaxy (NLS1) 1H0707-495 was the first object to clearly show a reverberation delay (Fabian et al. 2009; Zoghbi et al. 2010). It is seen as a short lag between the direct power-law, dominating the $2-4$ keV band, and the soft excess < 1 keV, produced by the relativistic-broadening of the reflection spectrum. The short delays are due to the light path difference between the direct and reflected emissions in the vicinity of the black hole. Many other objects have since shown similar lags (Emmanoulopoulos et al. 2011; de Marco et al. 2011; Zoghbi & Fabian 2011; Kara et al. 2012; Fabian et al. 2012; Cackett et al. 2012).

These lags could be produced in another scenario (Miller et al. 2010), where their small values are an artefact of a large scattering

Send offprint requests to: A. Zoghbi

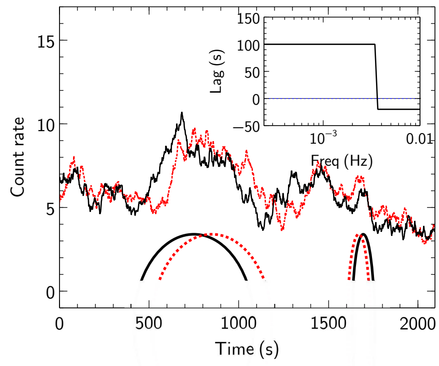

Fig. 1. A visual representation of the what the frequency-resolved lag mean in the light curve. The two light curves are shifted with respect to each other with the lag plotted in the inset as a function of frequency. At low frequencies, the first light curve (black continuous) leads, while the second (red dotted) light curve leads at high frequencies.

medium, the bulk of which is close to the line of sight. This is however not consistent with the spectroscopy and requires special geometries (Zoghbi et al. 2011). An inherent ambiguity in interpreting the soft excess itself remains however. Its smoothness requires in many cases extreme values for the fit parameters (Crummy et al. 2006). These values could indeed be real as we are studying extreme objects, but the greatest potential for removing such ambiguities is in studying the variability and reverberation in the iron K band.

2. Interpreting the lag

2.1. Frequency-dependent Lags

Time delays between light curves in two energy bands are measured using the phase of the cross spectrum (Nowak et al. 1999), giving the time lag as a function of Fourier frequency (or variability time-scale). The observed lags often show significant dependence on frequency, and that is the reason the classical cross correlation function does not isolate them.

Visualizing the frequency-dependent lags in the light curve is illustrated in Fig. 1 using simulated light curves. The plot shows two light curves delayed with respect to each other with the lag spectrum plotted in the inset. At low frequencies (long time-scales), the continuous black light curve leads, corresponding to a positive lag in the inset, while at high frequencies (small time-scales), the red dotted light curve leads.

Similar patterns have been observed in several NLS1, with several arguments pointing to two separate processes producing the positive and negative lags (Zoghbi et al. 2011). The observed negative lags (also called soft, because the soft < 1 keV band lags the hard $2-4$ keV band) are most likely due to reverberation at very small radii (a few $r_g = GM/c^2$) in the accretion disk. A strong evidence for this is the energy-dependence of the lag at those high frequencies discussed next.

2.2. Energy-dependent lag

In addition to the frequency dependence, the observed lags are also energy-dependent. So 2D plots are needed to capture the full lag behaviour (Zoghbi & Fabian 2011). Alternatively, the energy-dependence can be isolated for a single frequency band. Light curves are produced in several energy bands, then for every light curve, lags as a function of frequency are produced, taking one of the light curves as a reference. The lag is then plotted as a function of energy for the frequency of interest.

If the two light curves of interest contained contribution from individual components, the first band is *only* due to say direct emission, and the second band is *only* reflected emission, then the calculated lag is the intrinsic delay between the two components. This is however not the case in practice, where each band contains contribution from *both* components. Therefore, the calculated lag is the intrinsic lag, diluted by a factor representing the relative contribution of direct and reflected emission in each band. It turns out, the lag as a function of energy is closely related to the reflection fraction as a function of energy (e.g. Poutanen 2001).

Fig. 2 illustrates the effect of reflection fraction and the interpretation of lag-energy plots. On the left plot (a), the relative contribution of direct and reflected components is the

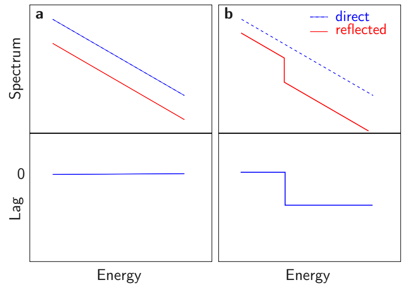

Fig. 2. A visual representation of the link between the spectrum reflection fraction and the lag-energy plots. Top panels show the spectra a direct and reflected components in arbitrary units. The bottom panels show the resulting lags as a function of energy assuming a constant lag between direct and reflection emissions.

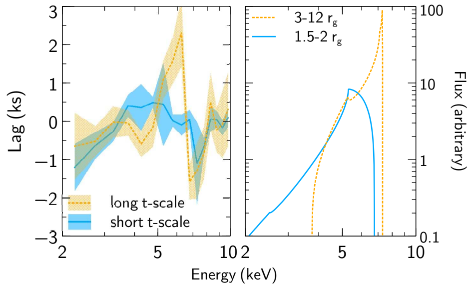

Fig. 3. Left: lag-energy plot for NGC 4151 for long (freq< 2×10^{-5} Hz) and short ($(5-50) \times 10^{-5}$ Hz) time-scales (Zoghbi et al. 2012). Right: the shape of a broad iron line emitted from two different regions, produced with the `laor` in xspec.

same in all bands, and so the measured lag as a function of energy is zero. It is when the reflection fraction changes, that the lag as a function of energy changes (right plot: b). Note also that the lag zero point depends on the chosen reference band. The plot b-bottom is for the case of taking the lowest energies as a reference. If instead the highest energies are taken as a reference, the lag plot would shift vertically so that the highest energies lag is zero.

3. Observed reverberation

As noted earlier, frequency-dependent lags have been seen in several AGN with a characteristic shape that is positive at low frequencies and negative at higher frequencies. It is the energy dependence of the lag that offers the clues to its full interpretation. The few NLS1 whose lag has been studied as a function of energy show interesting trends. **At low frequencies**, the lag increases with energy, similar to what is well known in Galactic BH binaries. If interpreted as due to reflection, it implies an increase in reflection fraction with energy. This interpretation is clearly ruled out for Galactic BH binaries (Kotov et al. 2001). If their origin in AGN in the same, then reflection can be ruled out too. These low frequency lags are consistent with Comptonization or propagating fluctuations in the disk, although the picture is not fully clear.

At high frequencies, where negative lags are seen, the energy dependence of the lags has a different shape. In the $0.3-10$ keV band, it has a minor peak first at 0.7 keV, it then decreases with energy reaching a minimum at ~ 2 keV, then increases again. This shape indicates that the reflection fraction has the same pattern, which is in fact well known from spectroscopy. A partially ionized reflector produces exactly the same characteristic shape that, when compared to the illuminating power-law, it has a minimum at $\sim 2-3$ keV.

4. Iron K reverberation

Although the lag-energy shape could not be constrained at 6 keV for the objects studied initially (e.g. 1H0707-495, IRAS 13224-3809 and RE J1034+396 and others) due to the low counts at those energies, looking at other bright objects at 6 keV revealed the continuation of the pattern. Zoghbi et al. (2012) showed that there is indeed a delay between the peak of the iron K line ($6-7$ keV) and the wings of the line. The shape of the lag as a function of energy resembles a broad iron line (Fig. 3).

The fact that there are features at $\sim$ 6 keV in the lag is a clear indication that it is due to reflection. It cannot be due to the narrow Iron K line usually seen in AGN because that fails to explain the lags at soft energies in many NLS1. The lag therefore has to be due to a relativistically-broadened iron line produced by reflection in a partially ionized reflector. The same reflector is also responsible for producing the soft excess and the lags seen < 1 keV in NLS1.

Furthermore, detecting lags in the Fe K band, a clean and better understood part of the spectrum, allows us to go beyond detection and start to probe the emission region itself. Fig. 3-left show the lag-energy plot for two time-scales for NGC 4151 (see Zoghbi et al. 2012, for details). First, as noted earlier, there is a clear broad line-like feature that peaks at 6 – 7 keV, but more interestingly, the width of the feature seems to change with time-scale. The time-scale of the variability gives, in the simplest interpretations, a measure of the size of the emitting region. Long time-scales are associated with large emission regions, and most likely larger distances from the central object, while smaller time-scales are more likely to be associated with smaller radii. The shape of the lag with energy is in full agreement with this picture. As noted earlier, the lag-energy plot gives a measure of the reflection fraction, so the shapes in Fig. 3-left represent roughly the shape of the relativistically-broadened line produced by reflection. Relativistic effects produce a red wing that extends to lower energies and blue horn at energies higher than the rest energy of the line. This shape changes depending on the radius at which most of the emission originates and is illustrated in Fig. 3-right. As can be seen, the change in shape resembles the change in the lag with time-scale. So here, we are seeing emission coming from different regions in the accretion disk, each responding differently to variability in the illuminating continuum.

5. Conclusion

X-ray reverberation in AGN is emerging as an important tool to probe the vicinity of supermassive black holes, promising a better understanding of these environments in the near future. Iron K reverberation is particularly interesting, as it probes a clear part of the spectrum that is better understood. The results of NGC 4151 has shown some of the early possibilities of what can be done. There are now more objects that show similar results (Zoghbi et al. ApJ submitted), which will help contextualize and generalize the results.

Acknowledgements. This article is based on published work done with many collaborators, including: C. Reynolds, A. Fabian, E. Cackett, P. Uttley and others.

References

Cackett, E. M., et al. 2012, ArXiv e-prints
Crummy, J., Fabian, A. C., Gallo, L., & Ross, R. R. 2006, MNRAS, 365, 1067
de Marco, B., et al. 2011, MNRAS, 417, L98
Emmanoulopoulos, D., McHardy, I. M., & Papadakis, I. E. 2011, MNRAS, 416, L94
Fabian, A. C., et al. 2012, ArXiv e-prints
Fabian, A. C., Rees, M. J., Stella, L., & White, N. E. 1989, MNRAS, 238, 729
Fabian, A. C., et al. 2009, Nature, 459, 540
Kara, E., et al. 2012, ArXiv e-prints
Kotov, O., Churazov, E., & Gilfanov, M. 2001, MNRAS, 327, 799
Miller, L., Turner, T. J., Reeves, J. N., & Braito, V. 2010, MNRAS, 408, 1928
Nowak, M. A., et al. 1999, ApJ, 510, 874
Poutanen, J. 2001, Advances in Space Research, 28, 267
Reynolds, C. S., Young, A. J., Begelman, M. C., & Fabian, A. C. 1999, ApJ, 514, 164
Ross, R. R. & Fabian, A. C. 1993, MNRAS, 261, 74
Zoghbi, A. & Fabian, A. C. 2011, MNRAS, 418, 2642
Zoghbi, A., Fabian, A. C., Reynolds, C. S., & Cackett, E. M. 2012, MNRAS, 422, 129
Zoghbi, A., et al. 2010, MNRAS, 401, 2419
Zoghbi, A., Uttley, P., & Fabian, A. C. 2011, MNRAS, 412, 59